23

Bridge Maintenance Management System for Egnatia Motorway

Authors:
Eleni Sakoumpenta
Panagiotis Panetsos
Manolis Haralabakis

Motivation

The feasibility of the application of the IRIS risk paradigm in case of multi-hazards, namely an active landslide in an earthquake prone region, is of interest for assessment. A proof of concept is desired.

Main Results

A monitoring system has been installed at the T11 Bridge within the Egnatia motorway in Northern Greece. The successful application of the new IRIS Risk Paradigm has been demonstrated.

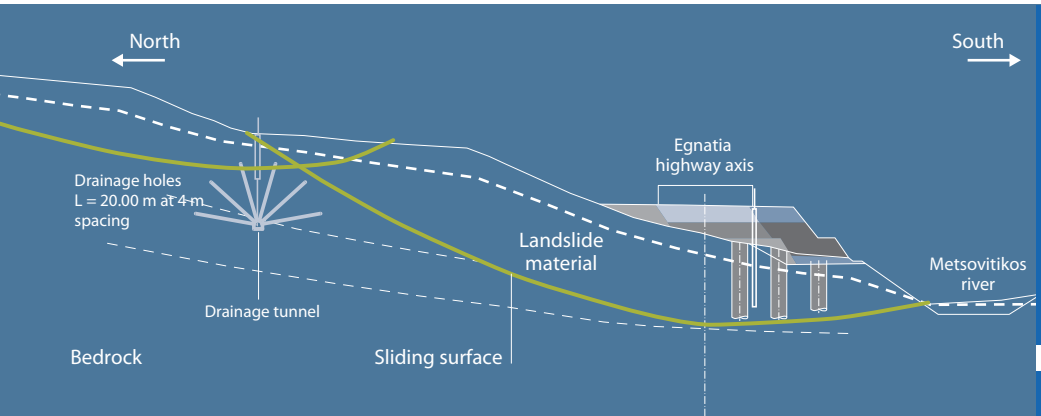

23-1 Introduction

The T9/T11 ravine bridge is located on Egnatia motorway in northern Greece approximately 100 km east of the Adriatic port of Igoumenitsa and 240 km west of Thessaloniki (F.23-1). The motorway in this area runs at a very short distance from the north side of Metsovitikos river. Due to severe geotechnical problems that prevail in this particular area, extensive geological and geotechnical investigations were carried out and several alternative alignments on both sides of the river have been examined. The current alignment was selected as the one that exhibits the least residual geotechnical risk among the other alternatives, however, still not negligible.

The bridge consists of two separate structures, one on each carriageway: T9 on the right carriageway (west-east direction) and T11 on the left. T9 is a 409 m long four-span structure (44 m + 105 m + 155 m + 105 m) monolithically connected on piers M1 and M2 and supported through elastomeric bearings on abutments A1 and A2 and the western pier Ma (F.23-2). T11 is a 365 m long, three-span, continuous structure (105 m + 155 m + 105 m) monolithically connected on piers M1 and M2 and supported through elasto-

Structure location F.23-1

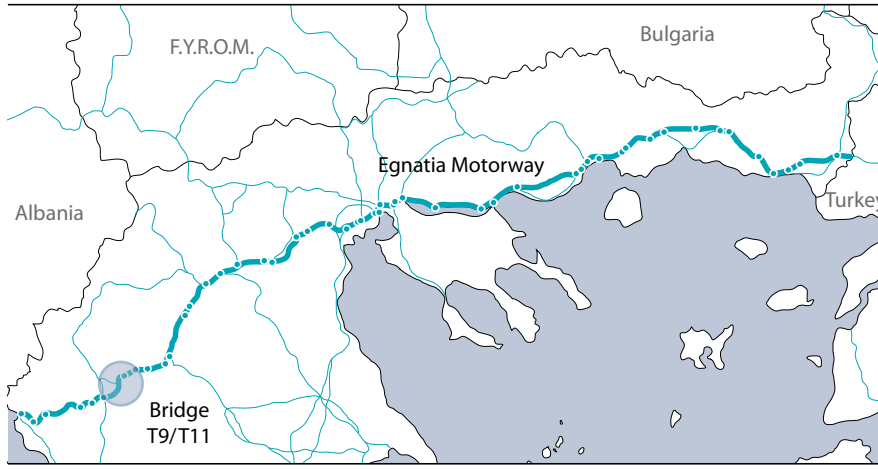

View of T9/T11 bridge F.23-2

Longitudinal section F.23-3

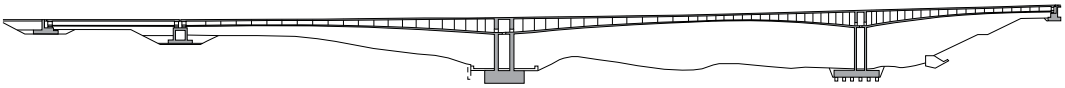

meric bearings on abutments A1 and A2. The bearings are freely sliding in the longitudinal direction and the deck is transversely restrained through hydraulic viscous dampers on abutments and pier Ma. The width of each carriageway is 14.45 m. The deck is a box-girder ranging in height from 4.00 m (midspan) to 10.74 m, (pier supports) longitudinally pre-stressed through internal tendons and constructed with the free balanced-cantilever method.

The pier walls have a hollow rectangular cross-section and a maximum height of approximately 27 m (pier M2). The foundations of piers M1 are rock-sockets whereas of piers M2 there are groups of 1.5 m diameter piles. The foundations of abutments A1 and A2 and pier Ma are spread footings (F.23-3).

The particular feature of bridge T9/T11 is that, unlike piers M1 and M2 which are founded on stable ground, the bridge abutments and pier Ma are founded on active landslide areas (areas A and B1 in F.23-4). According to monitoring data, from inclinometers installed during the design stage, the depth of the sliding surfaces was approximately 25-30 m and the maximum recorded rate of ground movements 30 mm/month. The groundwater level is high and artesian water pressure has been observed in some boreholes. Major stabilization works have been implemented in order to minimize the risk of sliding movements. However, as the risk of sliding movement cannot be completely eliminated, the bridge has been designed to undertake vertical (–10 cm/+3 cm) and horizontal (20 cm) movements at the abutment locations under static conditions induced by slow soil creep or seismic loading. Detailed description of the geotechnical conditions and the stabilization works are included in chapter 23-2-1.

The construction of the bridge has been completed in the beginning of 2010.

Landslide areas at abutment areas (area A at the west abutment, area B1 at the east abutment) and vectors of the ground movements F.23-4

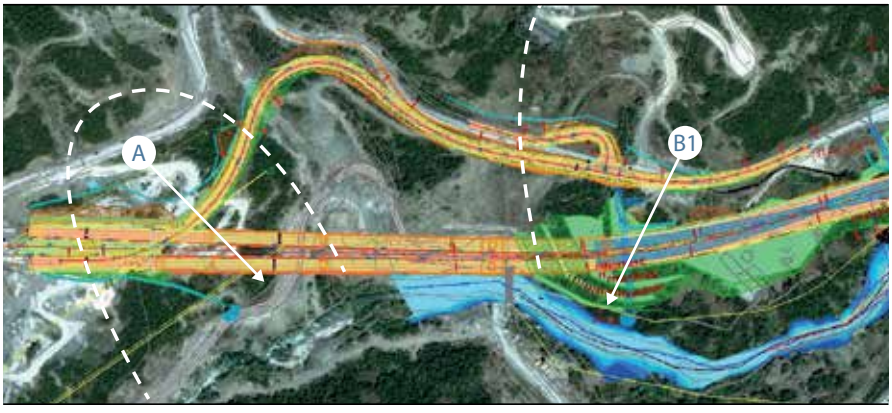

The aim of this report is to describe the application of the Risk Paradigm methodology for the geotechnical risk assessment of the abutment areas and the risk assessment of the bridge and to discuss its results.

23-2 Geotechnical Risk Assessment of Abutment Areas

23-2-1 Geotechnical Conditions

In the area of the T9/T11 bridge, the motorway runs at a very close distance along the main front of a huge overthrust of the Pindos Unit formation, comprising mainly flysch, over the Ionian Flysch. The tectonic movements associated with it have resulted in stressing of the formations and a consequent degradation of their mechanical properties. Therefore, the geology in the area is very complex and chaotic, containing randomly orientated shear faults with locally weak surfaces, low strength rock masses and landslides of various sizes. The groundwater table is generally high due to the low permeability of the soil and rock formations and the high precipitation received in the area.

The selection of the alignment in this area was an issue of great concern for EOAE. Numerous alternative alignments were investigated during the course of finalizing the highway design. Originally, it passed through the slope south of the river but ground investigation and monitoring with inclinometers indicated that the slope is creeping at a depth in excess of 80 m with a rate of about 18 mm/year. This finding led to the abandon-

Plan with structure location and landslide areas A and B1 F.23-5

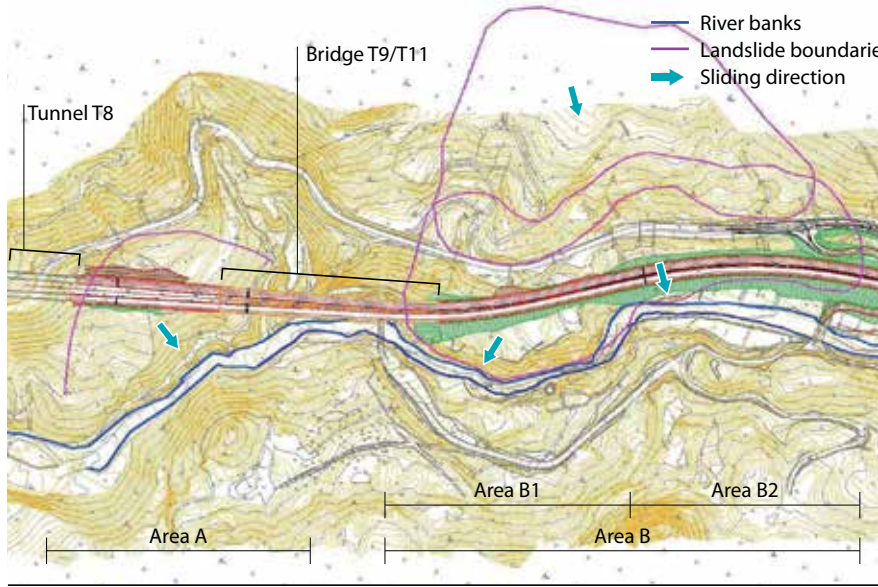

ment of the south side of the valley. As the findings of an initial borehole programme revealed, together with the installation of inclinometers and subsequent monitoring, creeping ground also existed north of the river but, in comparison, the ground conditions were overall more favourable: the observed movements were taking place at a much shallower depth, not exceeding 50 m. On average, the depth of movements was less than 20–25 m. A new set of alternative alignments was examined north of the river to establish the safest corridor for the motorway. It was concluded that the alternative that posed the lowest risk was to construct the motorway on embankment at the toe of the valley side and close to the river in order to: a) achieve buttressing of the landslide with the embankment and b) minimize the disturbance of the weak, sliding material.

It should be noted that, during the process of finalizing the highway design, a panel of international experts was employed by EOAE to support the evaluation of the geological-geotechnical investigation results and to endorse the final decision.

The geotechnical conditions for each abutment area and the adopted stabilizing measures are described below.

West Abutment (Area A)

Area A measures approximately 200 m by 300 m in plan and lies between the exit portal of tunnel T8 and the beginning of ravine bridge T9/T11 (F.23-5). The western abutment and one pier of the bridge are founded on spread footings within the area of instability. In total, more than 60 boreholes were drilled during different stages of the design. Of these, 20 were equipped with inclinometers and 32 with Casagrande and vibrating wire piezometers. The ground consists of an upper layer of old landslide debris comprising stiff sandy clay and medium to very dense clayey sand with gravel to a depth of 10–15 m in a chaotic and non-layered structure overlaying the tectonic mélange from the Pindos overthrust with a similarly disturbed structure but with stronger soil material. Bedrock is encountered at a depth of 30–35 m and comprises siltstone, sandstone and conglomerate. The groundwater regime is very complex, since water was found at varying levels in all boreholes. It appears that there are numerous perched horizons, while there are indications of seasonal artesian water locally. Overall, water is considered to play a major role in destabilizing the slope.

The depth of the sliding movement along the cross-section at the abutment location is about 12–15 m at the boundary between the landslide debris and the tectonic mélange formation. The maximum depth of movement in the area was measured at 25 m (inclinometer B6) within the tectonic mélange formation. Its rate, before construction, averaged at about 5 mm/year. Back analyses on two representative sections and ring shear tests were carried out to determine the most appropriate residual angle of internal friction, φ_{res}. The results varied between 13° and 17°, values subsequently adopted in the design of the stabilization measures.

Due to geometric restrictions on the alignment posed by the adjoining structures (tunnel T8 and bridge T9/T11) and the river, as well as the steep morphology and limited space at the toe of the landslide, a counterweight which is generally considered preferable as a stabilization measure could not be adopted. Instead, it was decided to construct three drainage tunnels with an array of 20-metre-long drainage holes through them under the entire area as shown in F.23-6. The works were completed in October 2007.

Cross-section showing the sliding surface and the stabilizing measures at the west abutment F.23-6

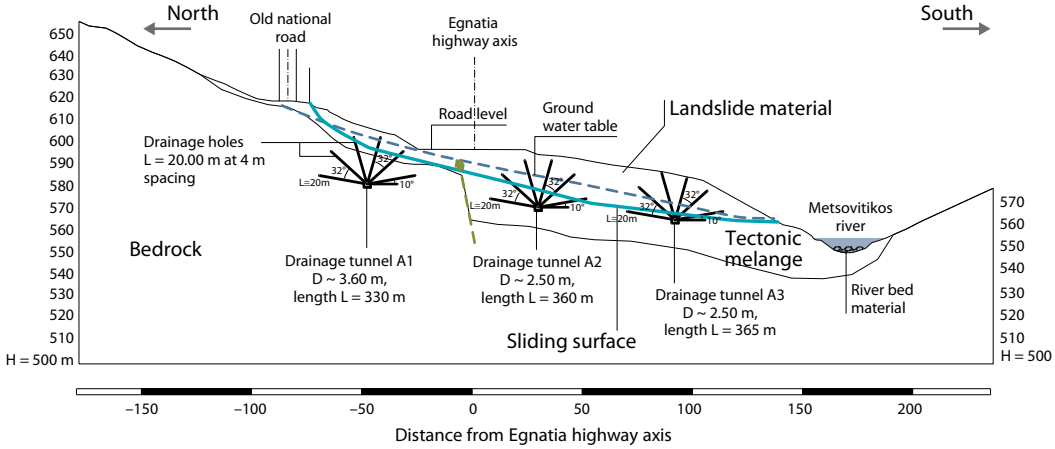

Although the results of monitoring in this area clearly show that the three drainage tunnels are very effective in reducing the rate of movements to practically zero, there is always a risk that, in the long-term, the drainage holes in the tunnels may fail to function which would lead to an increase of pore pressures in the ground and therefore to the triggering of an instability. This instability would seriously affect the maintenance cost not only of the approach embankment of the bridge but of the structure as well. Moreover, an earthquake loading presents also a great risk of instability in the area. The risk of such instabilities following the risk paradigm methodology is assessed below. Moreover, the horizontal displacements of the west abutment are computed through numerical analyses for various ground water scenarios in order to assess whether and to what degree potential deformations due to ground water rising could affect the bridge superstructure.

East Abutment (Area B1)

To the east of the ravine bridge, there is an extensive area of instability about 450 m long by 700 m divided in areas B1 and B2 (F.23-5). In the framework of this report, the interest is focused in area B1 where the eastern abutment of the bridge is situated. The abutment is founded on a 20-metre-high reinforced earth embankment within the unstable area, followed by motorway embankment with a height varying between 3 and 6 m. A total of 45 boreholes were drilled in this area, 19 of which are equipped with inclinometers and 23 with piezometers (Casagrande and vibrating wire).

The surface is covered by clayey and sandy material with gravel and a maximum thickness of 50 m, generally varying from 10 m to 30 m, identified as old landslide material. This is underlain by the completely weathered zone of bedrock, which is a soil–type material with highly variable percentages of clay, silt, sand and gravel, stiff/very stiff or medium dense/dense, with an average thickness of 15–20 m. Finally, bedrock comprises fractured and slightly weathered siltstone, sandstone and conglomerate. Across most of area B1, a

layer of sandy gravel and cobbles was found at approximately river level, having a thickness of about 4 m. This is believed to be part of the river bed before it was buried under the creeping soil mass. Moreover, large limestone boulders originated from the far uphill area of the natural slope slid downhill and piled up at the toe of the natural slope by the river bed. The groundwater table was found at a depth of 5–10 m, contributing significantly to the instability of the area.

Two retrogressive landslides is the prevailing movement mechanism as shown in F.23-5 and F.23-8. The lower one daylights at the river and destabilizes the upper one which, in turn, exerts destabilizing forces to the lower one and extends 450 m above the river. The maximum depth of movement is 45 m, while the average rate of movement was about 10 mm/year. Back analyses and ring shear testing were carried out to derive the shear strength along the slip surface. A representative value of $\varphi_{res} = 20°$ was adopted in the design. The alignment runs parallel to the river at the toe of the landslide. The thickness of the sliding material at the embankment foundation varies from 5 m to 40 m which, in combination with the presence of the river at the toe, makes its removal and replacement with high quality granular material impracticable. The embankment was therefore founded on creeping material at the toe of the lower landslide, acting as a stabilizing berm. However, the embankment alone was not sufficient to achieve the required safety factor of 1.40. In addition, the safety factor in local stability for random surfaces at the toe was inadequate.

As a result, additional measures to improve stability conditions under all modes of failure were designed. These included a drainage tunnel in the upper landslide, gravity drainage wells in the lower landslide (locally, in area B1, where river gravel was found) and reinforced concrete diaphragm elements in the foundation of the embankment (barrettes) in order to increase the stability of the reinforced embankment to an acceptable level. These are schematically shown in F.23-7 (plan) and F.23-8 (cross-section) and were completed by the end of 2009.

Although the monitoring results in this area clearly show that the stabilizing measures are effective in reducing the rate of movements to practically zero, there is always a risk

Plan with stabilization measures in area B F.23-7

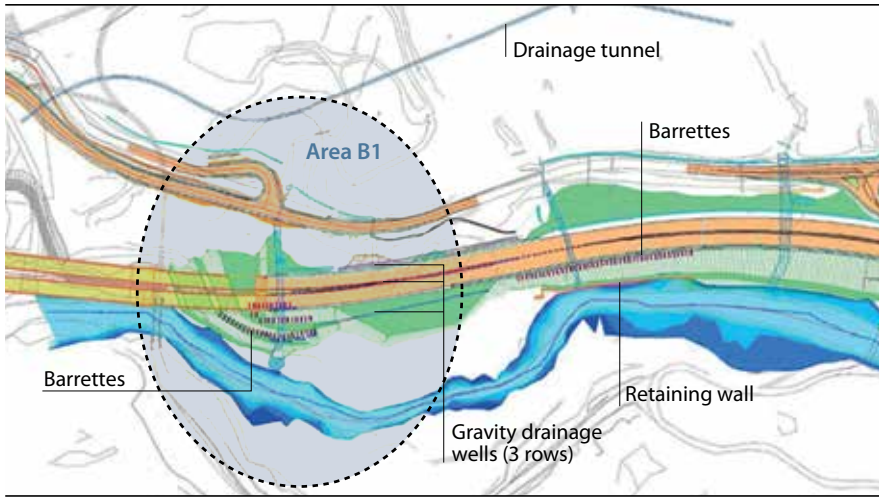

Cross-section showing the sliding surface and the stabilizing measures at the east abutment F.23-8

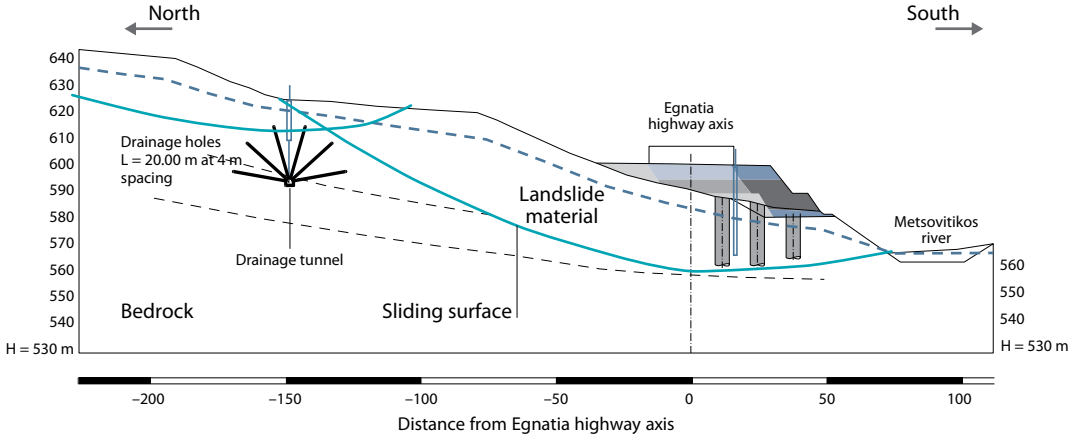

that, in the long-term, the drainage holes in the tunnel and the drainage wells may fail to function which would lead to an increase of pore pressures in the ground and therefore to the triggering of an instability. This instability would seriously affect the maintenance cost not only of the approach embankment of the structures but of the structure as well. Moreover, an earthquake loading presents also a great risk of instability in the area. The risk of such instabilities following the risk paradigm methodology is assessed below. Moreover, the horizontal displacements of the west abutment are computed through numerical analyses for various ground water scenarios in order to assess whether and to what degree potential deformations due to ground water rising could affect the bridge superstructure.

23-2-2 Geotechnical System Modelling

The risk of this system is a slope failure. The slope stability is checked through Limit Equilibrium Analysis (LEM) on a high number of potential circular slip surfaces. The performance function of the system is the Factor of safety (FoS) which is the sum of the resistance forces over the driving forces along an examined surface. Failure occurs when the driving forces exceed the resistance forces, i. e. when FoS is less than unity. Therefore, the risk consequence measure $h(\boldsymbol{\theta})$ is equal to an indicator function $I_F(\boldsymbol{\theta})$ which is defined as follows:

$$I_F(\boldsymbol{\theta}) = \begin{cases} 0 & \text{if failure does not occur, i.e. FoS} \geq 1 \\ 1 & \text{if failure occurs, i.e. FoS} < 1 \end{cases} \quad \text{E.23-1}$$

where $\boldsymbol{\theta}$ is the model parameter vector that integrates all the uncertainties involved in the occurrence of the failure. It should be noted that here the risk corresponds to the probability of failure of the system.

The model parameter vector is composed of the parameters of the excitation model ($\boldsymbol{\theta}_f$), the system model ($\boldsymbol{\theta}_m$) and the performance evaluation model distinguished in the component ($\boldsymbol{\theta}_c$) and impact ($\boldsymbol{\theta}_i$) model. In this case, the excitation model comprises the pore pressure and the earthquake loading. These are related to the ground water table and the seismic ground acceleration respectively. The system model consists of the following three parameters: the unit weight γ, the effective friction angle φ' and the effective cohesion c′ of each soil layer. A number of geotechnical instruments (piezometer and inclinometers) have been installed in order to monitor the behaviour of the system. The role of these instruments is twofold. In the design stage, the piezometer data served to accurately define the ground water table whereas the inclinometer data served to accurately identify the mechanism (geometry) of failure. Hence, some uncertainties related to excitation and model parameters are eliminated. During the design life of the motorway, the piezometer data contribute to assess the risk in real time by introducing in the model the actual ground water level whereas the inclinometer data to early detect any triggering of shear failure and therefore, the appropriate corrective measures to be timely applied. Finally, the impact vector has no elements since in this case the risk consequence measure $h(\boldsymbol{\theta})$ is equal to the risk performance measure $I_F(\boldsymbol{\theta})$ as defined in the E.23-1. The components of the model parameter vector are illustrated in F.23-9.

The geotechnical model in each area was defined from the results of the geological mapping and geotechnical investigation and monitoring. More specifically, the type and thickness of the various layers were defined from the data retrieved from the boreholes. The values of the strength parameters of these layers were determined following a statistical analysis of the laboratory test results. The sliding surface geometry (depth, shape etc.) was determined from the inclinometer readings whereas the ground water surface was established from the piezometer readings. The values of the strength parameters on the sliding surface were defined through back analysis (setting a factor of safety, FoS, equal to unity) and represent residual values since they have been developed after a high level

Model parameter vector F.23-9

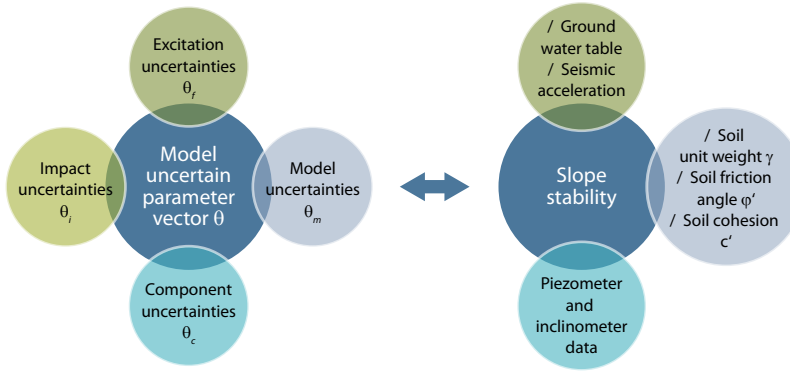

of shear deformation. The constructed stabilizing measures achieve to increase the FoS along the sliding surface from a value of 1 to a value of 1.3 and 1.47 for areas A and B respectively so that the motorway is safely accommodated.

All the LEQ stability analyses of this report were performed with the software SLIDE (Rocscience Inc.) adopting the Bishop simplified method.

23-2-3 Seismic Risk Assessment of Egnatia Bridges

One of the major risks that affect the serviceability and the integrity of the bridges and the structures of the Egnatia motorway is the seismic risk. The most of the bridges of the motorway are built in seismic prone areas. Although the Egnatia bridges are designed and built according to the latest national seismic code and in some cases according to more unfavourable site specific earthquake spectra, a catastrophic seismic event that could lead to major damages on some of the more vulnerable bridges cannot be excluded.

To identify sections of the road most at risk from seismic activity, to assess the damage resulting from various earthquake scenarios and to make emergency plans for the after-shock situation, data from a number of sources and analyses of individual structures or road sections were carried out. As the deterioration rhythm of various bridge components is predicted by the E_BMS model (the bridge management software of Egnatia Odos SA) or other well known curves which consider only the environmentally induced mechanisms, the assessment of the minor or even moderate damage expected from seismic events of smaller return periods, is useful for updating accordingly the life maintenance cycles adopted for the Egnatia bridges, for predicting unexpected seismically induced damages and repairs. Herein the seismic risk assessment was carried out for determining the bridges of Egnatia most at seismic risk for IRIS purposes.

Predefined grid for calculating Egnatia seismic hazard model F.23-10

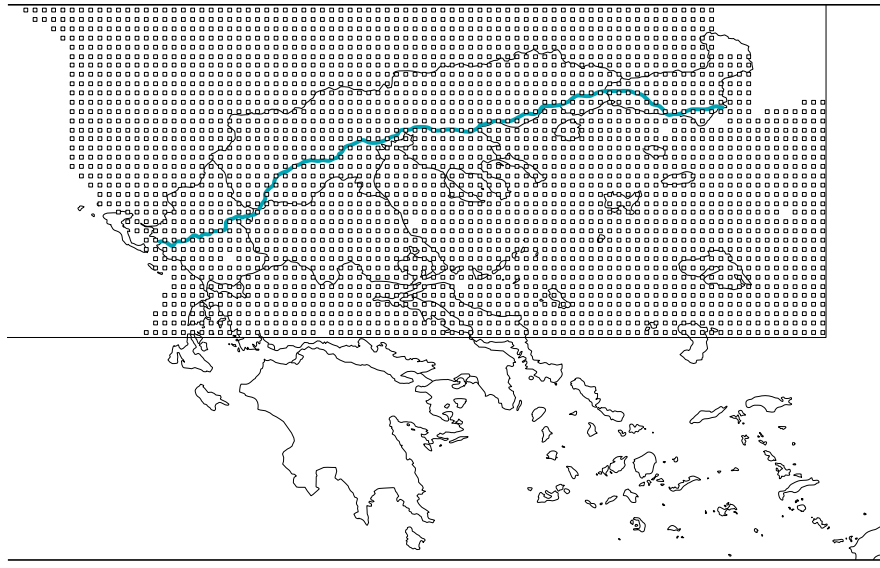

The Egnatia model. Seismic zones around the motorway, used by the Egnatia software F.23-11

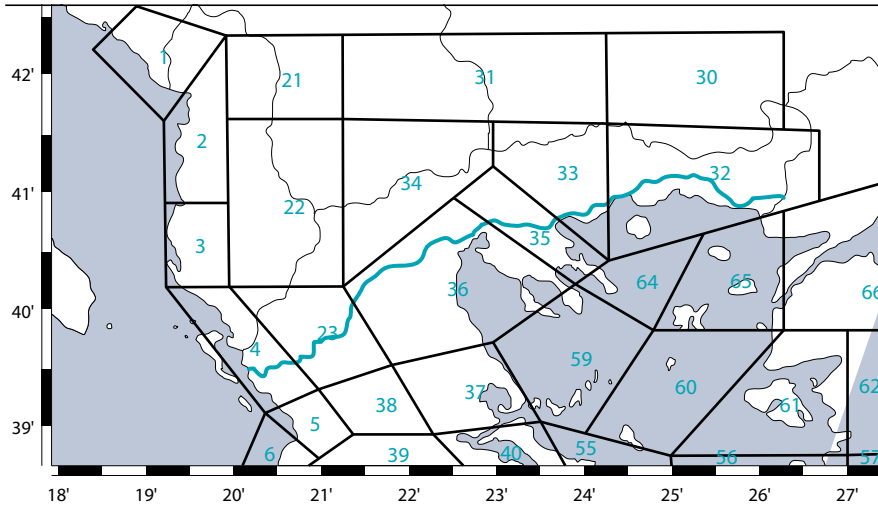

Seismic Hazard Model of Egnatia Motorway

A seismic hazard model, considering historical data for each of 66 zones across the region surrounding the Egnatia road, was prepared by the Greek Institute of Technical Seismology and Earthquake Engineering [Theodoulidis, 2001] and defined: The frequencies of earthquakes of different magnitudes at different points on a pre-defined grid, covered the area shown in WD-471, with grid points spaced at intervals of 0.1°. At each grid point seismic data for magnitudes from 4.5 to 8.5 in 0.25 increments and at varying hypocentral depths were provided. An attenuation relationship for northern Greece was adopted after considering all the historical data of the area.

Seismic Vulnerability Analysis of Bridges

Egnatia bridges were classified to eleven structurally representative categories depending on the structural types of the superstructure, the substructure and their interconnection. For these eleven structural types representing all the major bridges of Egnatia motorway, their seismic fragility curves were analytically derived. The result was a set of vulnerability functions, relating the damage estimate of a bridge (probability of exceeding a damage limit state) with the measure of the seismic intensity at the point-location of this bridge, representative of all the bridges of Egnatia motorway. Each vulnerability curve consists of a mean percentage damage plotted against the hazard intensity, and the associated standard deviation. Together these parameterise a distribution of damage at the given intensity. In T.23-1, the properties of the eleven representative bridge structural types are given.

In F.23-12 the main characteristic of the bridges selected to be analysed as representing the eleven structural types are shown.

Seismic Risk Assessment Software

The Egnatia motorway Authority has developed a software package to assess the vulnerabilities of structures along the motorway to seismic activity of an earthquake [EQE, 2001]. The software brings together data from a number of sources and analyses various

Main characteristics of the bridges for which the fragility curves were determined F.23-12

Structural configuration	Bridge name and class	No. of spans	Span length [m]	Total length [m]	Pier-to-deck connection	Curvature	Foundation
	Pedini Bridge 111	3	19.0 + 32.0 + 19.0	70.0	monolithic	in height	pile groups
	Siatista Bridge 311	3	16.25 + 30.5 + 16.25	63.0	monolithic	minor curvature in plan	pile groups
	T7 (section 14.1.2) Bridge 121	3	27.0 + 45.0 + 27.0	99.0	monolithic	no	footings
	G11 Bridge (right branch) 221	3	64.3 + 118.6 + 64.3	247.2	monolithic	in plan	caissons
	G9 (section 5.1) Bridge 421	2	85.0	170.0	monolithic	in plan	caissons
	Eirini Bridge 122	4	45.0	180.0	through bearings	no	pile groups
	Lissoss River Bridge 422	11	1× 29.56 + 3× 37.05 + 6× 44.35 + 1× 26.50	433.31	through bearings	no	pile groups
	2nd Kavala Ravine Bridge 232	4	42.0 + 2× 43.5 + 42.0	180.0	through bearings	no	caissons
	G2 (section 1.1.6) Bridge 332	3	30.7 + 31.7 + 30.7	93.1	through bearings	no	pile groups
	Kossynthos River Bridge 432	5	35.0 + 3× 36.0 + 35.0	178.0	through bearings	no	pile groups
	Krystallopigi Bridge 223	12	44.17 + 10× 54.98 + 44.17	638.19	monolithic/ through bearings	in plan	pile groups

Structural representative bridge types of Egnatia motorway T.23-1

Type	Code of the bridge	Number of bridges of the same type
Slab on single columns	111	15
Slab on multi columns	311	13
Boxbeam on single circ. columns	121	10
Box beam on single hollow rect. columns	221	30
Box beam on walls	421	12
Box beam on single columns (bearings)	122	10
Box beam on walls (bearings)	422	7
Precast beams on walls (bearings)	432	20
Precast beams on rect. hollow columns (bearings)	232	50
Precast beams on multicolumns (bearings)	223	5
Box beam on single hollow rect. columns (combination of bearings with monolithic)	223	30

bridges or motorway sections for probabilistic damage, or damage caused by real or theoretical seismic scenarios. The various inputs to the software are:

The two parts of the hazard model were combined to generate the shaking intensities for any bridge located in the grid, for any soil type and for a predefined return period.

The vulnerability functions are formulated in terms of the hazard intensity, which is ln(PGA) in the Egnatia software.

Egnatia software is used herein for the seismic risk assessment of all the bridges of Egnatia motorway, where for each of them a proper vulnerability function was assigned. Both options of the software were used for running probabilistic and user-defined scenario analysis for the selected bridges.

Probabilistic Analysis

A probabilistic analysis incorporates all major sources of shaking hazard, resulting in a probabilistic description of occurrence of the hazard intensity, through hazard curves. For each grid point, the frequency with which a certain intensity of shaking recurs is calculated. The program interpolates between grid points to calculate the shaking intensity at the precise location of the two bridges. The seismic intensity obtained automatically, incorporates the ITSAK soil model, while the model may be further modified by the specification of increments or factors considering new seismological data measured from recent seismic events, or more unfavourable site specific conditions.

Once the shaking intensity is estimated at a site, the induced damage to the structure is quantified using the vulnerability function of the specific bridge, which has been analytically derived for all the structurally representative bridge types of Egnatia motorway. The individual damage estimates for each possible event are probabilistically aggregated to estimate overall expected (annual) damage and associated uncertainty, as well as damage by return period.

Computation of damage for a bridge F.23-13

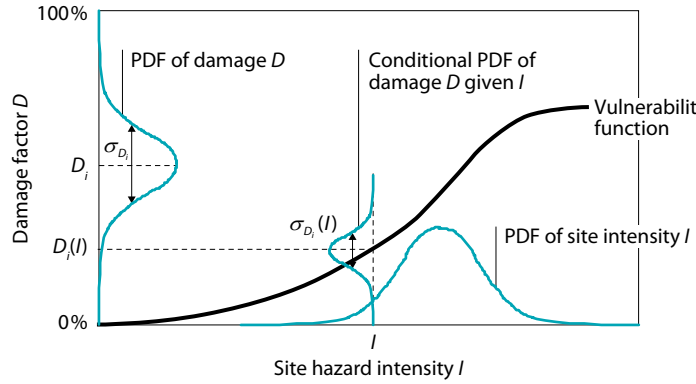

The hazard module will yield a probability density function of the shaking intensity at the site, as shown in the horizontal axis of F.23-13. For each value of the hazard intensity, I, a mean damage factor, $D_i(I)$ is obtained from the vulnerability function, with its corresponding standard deviation, $\sigma D_i(I)$. The result is a probability density function of the damage factor from which a mean value, D_i, and standard deviation, $\sigma D_i(I)$, for the damage factor of a particular structure, can be obtained. The expected damage is the sum over all events of the product of the mean damage for the event and the event frequency.

The damage distribution may be used to determine the probability of exceeding any particular level of damage. The frequency of exceeding this level of damage is obtained by multiplying the probability by the event frequency. Adding these damage frequencies across all events gives the total frequency of exceeding a given level of damage. If it is assumed that the arrival of earthquakes is a Poisson process, the annual probability of exceeding the level of damage can be calculated. Then the annual probability may be interpreted as a return period by taking its reciprocal. It is important to remember that this is the probability of exceedance smaller levels of damage that will also occur within the return period.

Damage Estimate

The output of the analytical module is a damage estimate for each structure. The damage estimate is provided as a percentage value and is written back into the "analysis_data" column in the Technical GIS. The results may be exported as a text file suitable for import into excel or word, or printed directly from the software. The exact meaning of a given "percentage damage" is discussed below.

Choice of Intensity Parameter

It was preferred to use vulnerability functions in PGA rather than MMI. Although attenuation relationships for intensity in both PGA and MMI were available from ITSAK, the vulnerability analyses carried out by Imperial College [Elnshai and Borzi, 2000] and later by [Moschonas et al., 2009], used PGA as a measure of intensity, and this choice has been

maintained in the software. From an engineering point of view, the damage suffered by an individual structure is directly related to PGA, not to MMI. PGA is a parameter that can be better related to the damage when vulnerability curves are derived analytically, as they have been for the Egnatia software. MMI is derived from the percentage of buildings suffering a given level of damage in an earthquake; it should not, therefore, be used as a measure of intensity in the analysis of a single structure. The analysis of single structures is the main use to which the Egnatia software will be put.

Vulnerability Curves Provided with the Software

Eleven vulnerability curves have been provided with the software for all the bridge structural types of Egnatia motorway by Aristotle University of Thessaloniki [Moschonas et al., 2009], while other five were provided by Imperial College [Elnshai and Borzi, 2000] and [EQE, 2001]. For the purposes of the IRIS project a new vulnerability function was analytically derived for bridge T9/T11, considering the updated characteristics of the bridge as are identified using ambient vibration monitoring and non catastrophic tests. The method used to incorporate these into the software is described below.

Incorporation of Bridge Analytical Vulnerabilities into the Software

The vulnerabilities provided by Imperial College and Aristotle University of Thessaloniki for the Egnatia software comprise curves that show the probability of reaching or exceeding a given limit state. Each limit state represents the boundary of post-earthquake damage conditions, which are related to a percentage of damage. Thus the quantitative description of damage provided by the software may be linked to a qualitative description of the state of the structure following an event. The vulnerability curves cannot be used directly by the software, but must first be translated to the form of curve required to provide an estimate of damage given a shaking intensity from the ITSAK hazard model.

Analytically derived vulnerability functions of Krystallopigi bridge (type 223), for four damage states, in longitudinal direction F.23-14

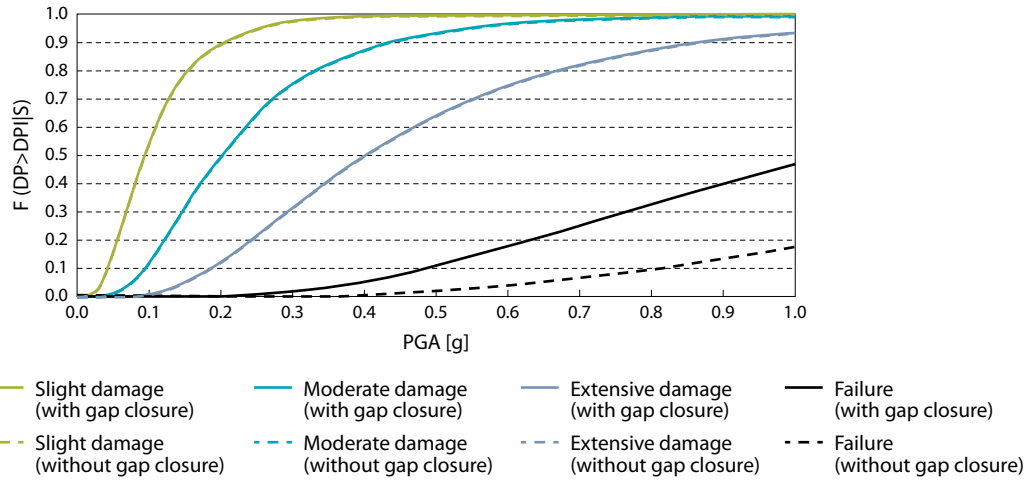

Quantitative representation of damage limit states T.23-2

Limit state	Level of damage	Repairs required	Damage %
1	No damage	No repairs	10
2	Minor damage	Limited repairs	30
3	Moderate damage	Extended repairs	45
4	Major damage	Partial repairs	60
5	Collapse	Replacement	100

This form of the vulnerability curve, which plots percentage damage against shaking intensity is derived from the Imperial College curves in the following way:

The probability of exceeding a certain damage state, but not exceeding the subsequent damage state are calculated, i.e. of being in a given post-event situation. For the example above, of the vulnerability function of F.23-14, derived by inelastic analyses of Krystallopigi bridge this gives:

Probability of exceeding limit state 1 but not reaching limit state 2 (P(LS1 < damage < LS2)) = 94 % − 62 % = 32 %, P(LS2 < damage < LS3) = 62 % − 22 % = 40 %, P(LS3 < damage < LS4) = 22 % − 2 % = 20 %, P(LS4 < damage < LS5) = 2 % − 0 % = 2 % (where LS5 is taken to be collapse).

Each limit state is associated with a range of percentage damage. The level of damage corresponding to limit states 1, 2, 3 and 4 (no, minor, moderate and major) damage are outlined in T.23-2.

The probabilities of exceeding a damage state but not exceeding the subsequent damage state can therefore be linked to the mean percentage of damage in that limit state. Therefore:

Damage for P(LS1 < damage < LS2) = ½(30 +10) = 20 %, damage for P(LS2 < damage < LS3) = ½(45 + 30) = 37.5 %, damage for P(LS3 < damage < LS4) = ½(60 + 45) = 52.5 %, damage for P(LS4 < damage < LS5) = ½(100 + 60) = 80 %.

The percentage damage for each hazard intensity is then calculated using:

$$\%\text{damage} = \Sigma\{P(LS_i) \times D(LS_i)\} \qquad \text{E.23-2}$$

where $P(LS_i)$ is the probability of exceeding limit state i but not reaching limit state i+1 and $D(LS_i)$ is the damage associated with limit state i, as defined above. The term "mean damage ratio" is equivalent to the %damage × 100. For the example above, the %damage respecting the peak ground acceleration with return period of 50 years, 0.245 g, is thus computed as follows:

$\%\text{damage} = \Sigma\{P(LS_i) \times D(LS_i)\} = \{((94-62) \times 20) + ((62-22) \times 37.5) + ((22-2) \times 62.5) + ((2-0) \times 80)\} / 100 = 36.1\,\%$.

The resulting analytical vulnerability curve for bridge type 332 provided with the software and translated following the previously described methodology is shown in F.23-15:

Using the Egnatia Risk Assessment Software the following probabilistic analysis results were derived in terms of four different seismic return periods: 50-year percentage damage, 100-year percentage damage, 475-year percentage damage, 1000-year percentage damage.

In F.23-17 the results of this probabilistic analysis for all the bridges of Egnatia motorway are given in terms of %damage. In F.23-16 the motorway sections most at seismic risk are projected in the map.

The results verify the high seismicity and therefore the high vulnerability of those bridges built in West Epirus Section as well as in Central Section. It is very important that according to the results, for small return periods (50 and 100 years) moderate damage is predicted for the bridges of these motorway sections. In some cases it is then necessary to consider the damage and repair of critical bridge components earlier than predicted by the typical deterioration curves adopted in Egnatia Life Cycle Maintenance Costs. Specifically for the major bridges of Egnatia motorway the results are given in the following tables.

Vulnerability functions for bridge type 332 for 4 limit states and the equivalent vulnerability functions in terms of damage %. Transverse direction F.23-15

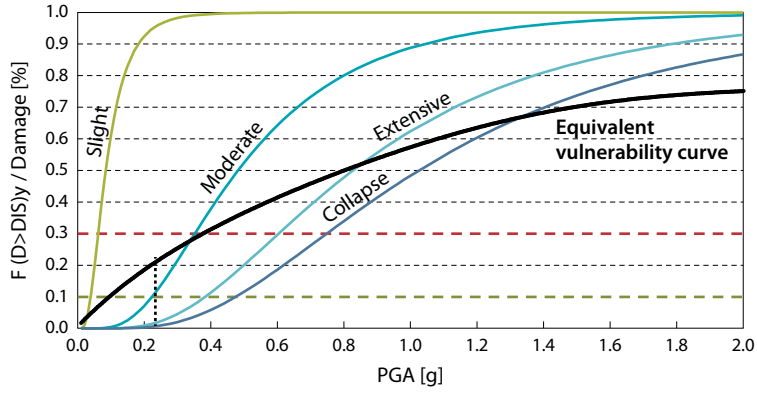

Egnatia motorway sections most at seismic risk F.23-16

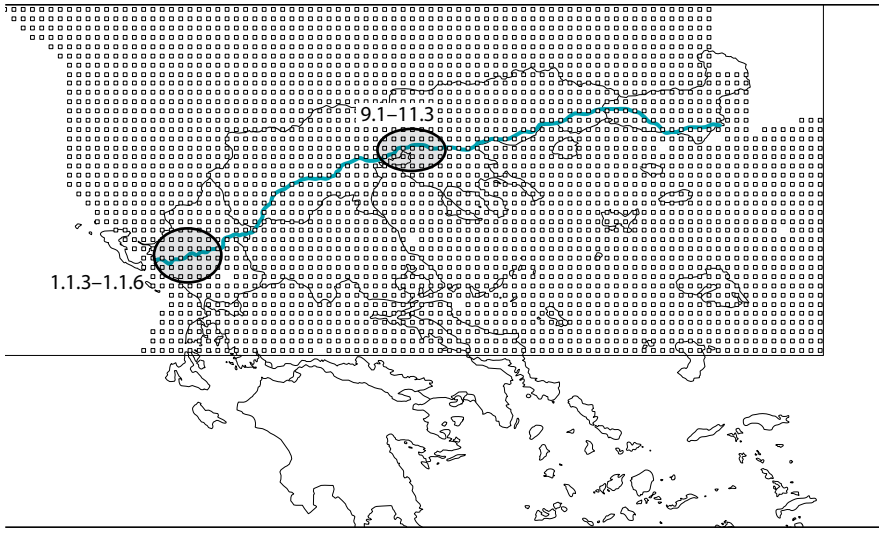

Distribution of probabilistic damages for Egnatia bridges for four return periods F.23-17

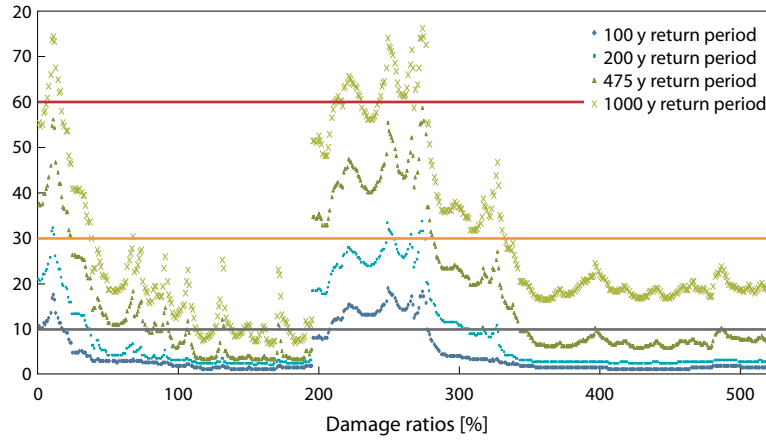

As it is shown in the last table, for some major bridges as Krystallopigi and Messovouni bridges in Epirus, or 5th Kavala bypass and Nestos bridge in the Central/East Sector of Egnatia, although their severe damage or collapse can be excluded as having small probability, their minor or moderate damage due to a seismic event having 100 % probability to happen once in the first 50 years of their life (50 years return period) has to be seriously considered as it will add repair expenses up to these already budgeted for the regular maintenance programme. In the case of Krystallopigi bridge the risk assessment is more unfavourable as it resulted in extended damage (>30 %) within the first 100 years of its total 120 years service life which would probably need extended partial reconstruction/ reinstatement other than this specified.

Seismic Risk Assessment of T9/T11 Ravine Bridge

In line with other similar procedures [FEMA-NIBS, 2004; Mackie and Stojadinovic, 2007], the fragility curve of bridge T9/T11 is analytically determined for IRIS project, following the proposed methodology described in previous paragraphs and expressed by the lognormal probability distribution function:

$$P_f(DP \geq DP_i \mid S) = \Phi\left[\frac{1}{\beta_{tot}} \cdot \ln\frac{S}{S_{mi}}\right] \qquad \text{E.23-3}$$

where $P_f(\bullet)$ is the probability of the damage parameter DP being at, or exceeding, the value DP_i for the i-th damage state for a given seismic intensity level defined by the earthquake parameter S (peak ground acceleration), Φ is the standard cumulative probability function, S_{mi} is the median threshold value of the earthquake parameter S required to cause the i-th damage state, and β_{tot} is the total lognormal standard deviation. The description of the newly determined fragility curve according to E.23-3 involves only two parameters, S_{mi} and β_{tot}.

Expected seismic peak ground acceleration for various return periods T.23-3

Bridge name	Return periods 50 y	100 y	475 y	1140 y
Metsovo Bridge	0.170	0.217	0.349	0.440
Aracthos Bridge	0.171	0.217	0.348	0.439
Polymylos Bridge	0.117	0.154	0.274	0.361
Krystallopigi Bridge	0.245	0.321	0.523	0.661
Mesovouni Bridge	0.254	0.324	0.524	0.662
5th Kavala Bypass	0.146	0.196	0.362	0.475
Greveniotikos Bridge	0.101	0.131	0.226	0.287
Votonosiou Bridge	0.139	0.176	0.286	0.356
Nestos Bridge	0.091	0.121	0.225	0.311

Expected seismic damage % for various return periods T.23-4

Bridge name	Return periods 50 y	100 y	475 y	1140 y
Metsovo Bridge	7.87	15.33	25.77	34.20
Aracthos Bridge	8.06	15.73	26.02	33.49
Polymylos Bridge	3.55	7.10	18.32	25.95
Krystallopigi Bridge	33.70	38.67	49.75	54.93
Mesovouni Bridge	22.34	26.88	37.89	45.36
5th Kavala Bypass	37.92	44.52	56.17	59.88
Greveniotikos Bridge	3.65	6.30	13.20	20.27
Votonosiou Bridge	7.65	10.27	20.25	25.97
Nestos Bridge	20.60	23.97	32.25	45.40

The first parameter is estimated on the basis of the capacity spectrum method, wherein the demand spectrum is plotted for a range of values of the earthquake parameter *S* (in spectral acceleration versus spectral displacement format) and it is superimposed on the same plot with the capacity curve of the bridge. The second parameter of E.23-3 is the total lognormal standard deviation β_{tot}, which takes into account the uncertainties in seismic input motion (demand), in the response and resistance of the bridge (capacity) which is governed by the uncertainty of the material stiffness and strengths, and in the definition of damage states. This parameter β_{tot} can be estimated by a statistical combination of the individual uncertainties (in demand, capacity, and damage state definition) assuming these are statistically independent. The value of β_{tot} was calibrated by [Dutta and Mander, 1998] using a theoretical approach and validated on the basis of empirical fragility curves obtained from actual bridge damage data gathered from the Loma Prieta (1989) and Northridge (1994) earthquakes. According to these studies the value of β_{tot} was set to 0.6; due to the lack of a more accurate estimation of uncertainties in capacity, demand and damage states, β_{tot} = 0.6 was used in the present study. For the purposes of the IRIS research project it was attempted to verify the uncertainty of the resistance of the bridge

Capacity spectrum method. For T9 (T > 0.5 sec) case 2 elastic demand spectra F.23-18

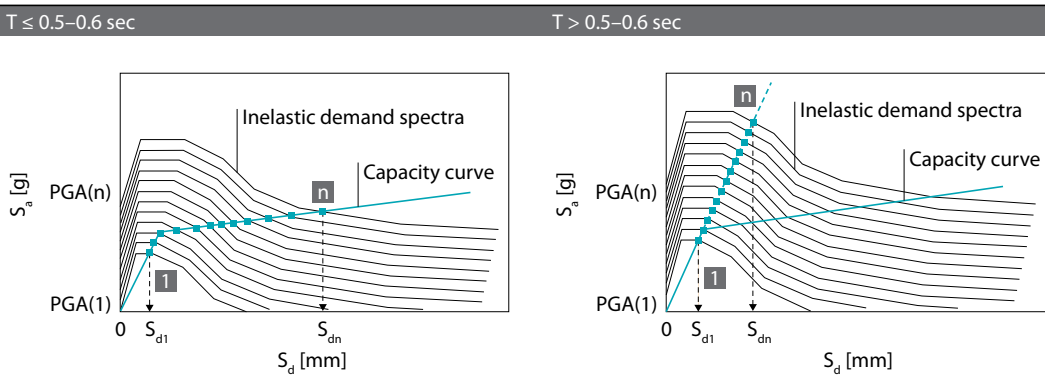

by statistically analyzing the big number of non catastrophic result Schmidt Hammer and ultrasonic tests. These two material concrete tests represent the basic properties affecting the non-linearities and the t is very important for determining the seismic capacity of the bridge to consider their uncertainty based on experimental data. The statistical analysis resulted to uncertainties well enveloped by the value of β_{tot} considered herein. The log-normal distribution gave a sufficient fit to the distribution of the test results. Therefore the consideration of the uncertainty by Dutta and Mander will be adopted once more for the fragility curve of T9/T11 bridge. The important issue here is that the properties of the nominal inelastic model for the T9/T11 bridge are updated based on the results of the ambient vibration monitoring. The values of the modulus of elasticity for the superstructure and the piers are considered equal to 1.0319 and 1.1177, or 38.75 Gpa and 38.00 Gpa respectively.

The capacity curve of the bridge was analytically determined by calculating the push-over curves using proper static inelastic modelling with the software package SAP2000NL V.14. In F.23-19 and in F.23-20 the analytic inelastic model representing the inelasticity as

3d inelastic model of the T9 Ravine bridge F.23-19

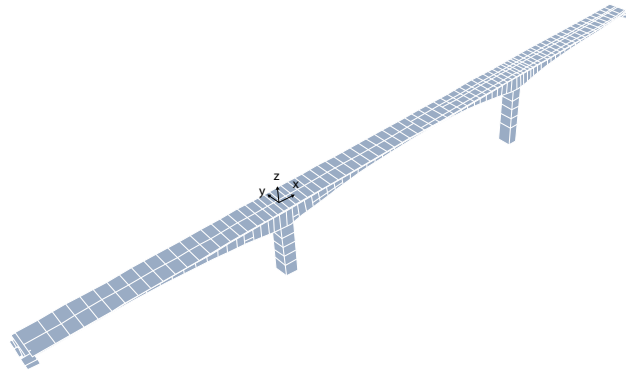

lumped with plastic hinges at both ends of the two piers M1, M2. The mechanism failure due to the formation of plastic hinges in both ends of the two piers is shown in F.23-20, with respect to the ultimate displacement of 0.56 m. The corresponding pushover curve representing the ultimate resistance up to the failure against earthquake is shown in F.23-21.

The final fragility curves representing the cumulative probability of exceeding the predefined damage limits states are shown in F.23-23.

The hazard model of Egnatia incorporated in the seismic assessment tool presented before in this paragraph, estimates the following peak ground accelerations for four different return periods, shown in T.23-5.

Projecting the probabilistic seismic intensities in terms of peak ground acceleration on the new fragility curve of T9 bridge the probabilities of exceeding various damage states can be predicted as shown in T.23-6.

Final failure pushover step (plastic hinges in both piers M1, M2 at the top and base sections) F.23-20

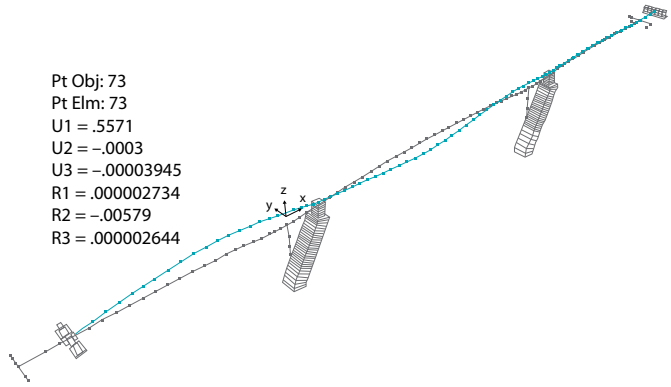

Plastic hinge properties of M2 base (left) and pushover curve (right) F.23-21

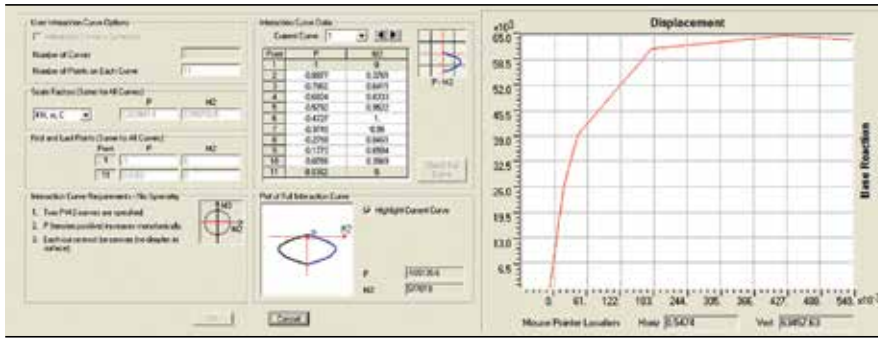

Fundamental longitudinal mode shape of T9 bridge (T = 0.94 sec > 0.5 sec) F.23-22

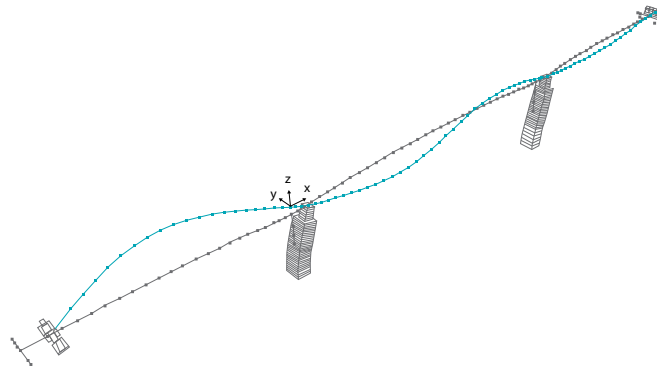

Seismic fragility curve for T9 bridge F.23-23

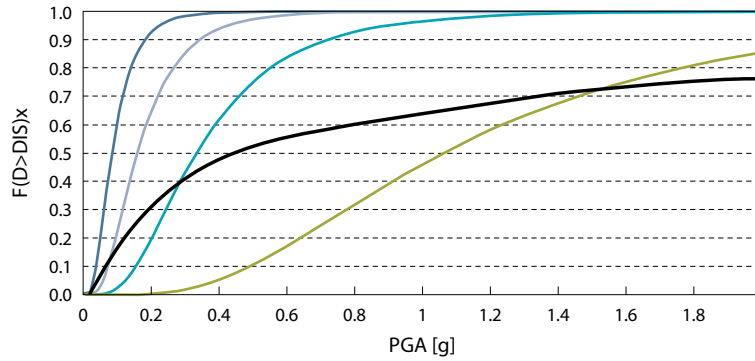

Expected seismic peak ground acceleration for various return periods on T9 bridge T.23-5

	Return periods			
Bridge name	50 y	100 y	475y	1140 y
T9/T11 Bridge	0.081	0.165	0.318	0.385

Predicted probability of different various damage states for four return periods, T9 bridge T.23-6

	Return periods			
Probability [%]	50 y	100 y	475 y	1140 y
Minor damage	6.598	37.41	78.02	86.25
Moderate damage	0.213	4.721	28.11	39.71
Extensive damage	0.000	0.260	4.491	8.441
Collapse	0.000	0.000	0.049	0.145

23-3 Progress beyond the Current Practice

A quantitative geotechnical risk assessment was carried out for very critical areas in terms of geotechnical instabilities for which only deterministic analyses were previously carried out. The assessment was carried out applying the IRIS Risk Paradigm methodology. For some failure modes, extremely high risk was calculated. In practice, monitoring data proved that modes of failures with very high calculated risk needed indeed further reviewing and additional stabilizing measures to lower the risk in tolerable margins. The residual risk was finally reassessed taking into account the implementation of the additional measures and the actual piezometer data. The final outcome highlighted specific aspects that need closer attention during the design life of the motorway.

The above actions have established a process to be followed in other areas of the motorway where critical geotechnical conditions may threaten the safety of the motorway. The quantitative estimate of risk supported by continuous monitoring will contribute to focus on areas that exhibit the highest residual risk and allow a proper maintenance plan to be developed and implemented in order to eliminate or mitigate it. The aim of the whole risk management process is to offer a safe motorway to the users with the least maintenance cost escalations.

Furthermore, the seismic risk assessment of major Egnatia motorway bridges and their pre and after shock management is to be upgraded incorporating the methodology developed in the frame of IRIS which combines statistical predictions with bridge models calibrated by experimental monitoring results. This results in a more accurate estimation of the probability to exceed various states of damages during their service life, which will help the maintenance authority to revise their currently adopted Life Cycle Costs, the type and the extent of their preventive measures, and the time of their implementation.

References

Dutta, A. and Mander, J.B., 1998. *Seismic Fragility Analysis of Highway Bridges, INCEDE-MCEER Center-to-Center*. In: Proceedings of the center-to-center workshop on earthquake engineering frontiers in transport systems, Tokyo, Japan, 311–325.

Elnshai, A.S. and Borzi, B., 2000. *Analytically Derived Vulnerability Functions for Egnatia RC Bridges*. Deliverable of Research Contract 330/A01/ΔM/EOAE, box no. S-224, September 2000.

EQE, 2001. *Seismic Risk Assessment Tool, Specification Document*. EQE International Ltd., Deliverable of Contract 330/A01/ΔM/EOAE, box no. S-225A/4/2001.

FEMA-NIBS, 2004. *Multi-Hazard Loss Estimation Methodology – Earthquake Model: HAZUSMH Technical Manual*. Washington, DC.

Theodoulidis, N., 2001. *Seismic Hazard Assessment along Egnatia Motorway*. Final Deliverable of Research Contract 406/A01/ΔM/EOAE., Box. No.S-243, May 2001.

Mackie, K.R. and Stojadinovic, B., 2007. *R-Factor Parameterized Bridge Damage Fragility Curves*. J Bridg Eng ASCE 12(4):500–510.

Moschonas, I. F., Kappos, A. J., Panetsos, P., Papadopoulos, V., Makarios, T. and Thanopoulos, P., 2009. *Seismic Fragility Curves for Greek Bridges: Methodology and Case Studies*. Bulletin of Earthquake Engineering, 7(2):439–468.